

# 이바노브-유리신 항복조건을 이용한 4절점 비선형 준적합 셸요소

## A nonlinear Co-rotational Quasi-Conforming 4-node Shell Element Using Ivanov-Ilyushin Yield Criteria

파노트 송삭 프라민<sup>1)</sup> · 김 기 두<sup>2)</sup>  
*Panot Songsak Pramin Kim, Ki Du*

요 약 : 유리신-이바노브 항복 조건을 이용하여 4절점 순수변위 준적합 셸요소의 정식화를 제안하였다. 기하강성 행렬은 그런 변형률 텐서를 이용하여 횡변형률 및 전단변형률도 기하강성행렬에 고려되었다. 그 결과 점선강성행렬의 해석적인 적분으로 비선형 해석시 매우 효율적으로 계산이 되고 있다. 이 정식은 변형률 경화의 이바노브-유리신 항복조건을 이용하여 재료 비선형 해석시에도 쉽게 적분이 된다. 즉 두께 방향의 적층 적분을 하지 않는 유리신-이바노브의 정식은 대규모의 셸 구조에도 계산상 아주 적합하다. 검증된 수치 예제에서 만족스러운 결과를 보여주고 있다.

ABSTRACT : Abstract. A co-rotational quasi-conforming formulation of four-node stress resultant shell elements using Ivanov-Ilyushin yield criteria are presented for the nonlinear analysis of plate and shell structure. The formulation of the geometrical stiffness is defined by the full definition of the Green strain tensor and it is efficient for analyzing stability problems of moderately thick plates and shells as it incorporates the bending moment and transverse shear resultant force. As a result of the explicit integration of the tangent stiffness matrix, this formulation is computationally very efficient in incremental nonlinear analysis. This formulation also integrates the elasto-plastic material behaviour using Ivanov-Ilyushin yield condition with isotropic strain hardening and its associated flow rules. The Ivanov-Ilyushin plasticity, which avoids multi-layer integration, is computationally efficient in large-scale modeling of elasto-plastic shell structures. The numerical examples herein illustrate a satisfactory concordance with tested and published references.

핵심 용어 :

KEYWORDS : 4-node shell, Quasi-conforming, Ivanov-Ilyushin

### 1. Introduction

The efforts of many investigators have been directed at overcoming the shear-locking problem in Mindlin-Reissner type 4-node shell elements, rendering the element effective and reliable for thin plate and shell applications. Simo and Rifai [1] developed a family of enhanced assumed strain (EAS) shell element formulation to improve the assumed strain shell element in the linear and nonlinear cases. The EAS shell element shows free

locking behaviour in thin shell and robustness in shell modeling.

Shi and Voyiadjis [2] presented a four-node quadrilateral C plate element with five degrees of freedom for geometric nonlinear analysis of plates. The element formulation was based on the updated Lagrangian formulation, the von Karman assumption and the quasi-conforming element method. The tangent stiffness matrix of the element was given explicitly without using numerical integration, which makes the element efficient for nonlinear analysis.

1) 건국대학교 사회환경시스템공학과 박사과정

2) 교신저자. 정회원, 건국대학교 사회환경시스템공학과 교수

(Tel. 02-970-7254, Fax. 02-948-0043, E-mail : kimd@konkuk.ac.kr)

본 논문에 대한 토의를 2008년 12월 31일까지 학회로 보내주시면 토의 회답을 게재하겠습니다.

Voyiadjis and Shi [3] extended their work to a non-linear shell element with five degrees of freedom per node.

In practical engineering problems, there is a need for a yield criterion in which the behaviour of the maximum collapse load of plates or shells is governed by plasticity. From literature reviews, there are two noted possibilities of working conditions: (1) in terms of stress which vary through the thickness of the shell in which case a yield criterion such as von Mises is used and (2) in terms of stress resultant in which Ilyushin's [4] or Crisfield's [5] yield criterions are used. The first attempt to reduce the rigorous efforts involved in plastic stress calculations using the shell thickness was made by Ilyushin [4]. He incorporated the resultant stress in the calculation of a perfect plasticity yielding and proposed a plastic yielding criterion which is then an explicit function of the resultant stress. Crisfield [5] improved this criterion by adding a pseudo hardening effect arising as a result of the progression of yielding across the shell thickness. Zeng et al. [6] extended this idea to isotropic hardening materials using approximate Ilyushin's [4] yield criterion with iterative algorithms to predict elasto-plastic resultant stress. In this case, the plasticity is managed by applying the von Mises yield condition and Plandtel-Reuss flow rule to discrete points throughout the thickness. The actual stress components are assumed to be the plane stress components at any level of the thickness.

The objective of this paper is to present the co-rotational formulation of a nonlinear 4-node shell element based on the quasi-conforming by Kim [7,8] and its application to elasto-plastic materials. The extension of Ivanov's yield criterion developed by Crisfield [5] to an isotropic hardening material is proposed in an explicit form of resultant stress. Numerical examples are also given for both Ivanov's and von Mises's yield plasticity. In comparison with the volume integration in plasticity, which are generally used in degenerated shell elements, the

computational time is significantly reduced for nonlinear analysis of shell structures.

## 2. GEOMETRY OF SHELL ELEMENT

The four node shell element shown in Fig. 1 is described by the local (r,s,t) coordinate whose origin is defined at the geometric center of the element. The geometric center of the element is determined by using the given global coordinates of the element nodes.

$$\mathbf{X}_c = \left( \sum_{i=1}^4 \mathbf{X}_i \right) / 4 \quad (1)$$

where  $X_c$  is the global coordinates of the center of the element and  $X_i$  is the global coordinates of node  $i$ .

The local coordinate system (r,s,t) is defined by first determining the vectors passing through the opposite midpoints of the shell mid-surface,  $l_1$  and  $l_2$ .

$$\mathbf{X}_{side\ i} = (\mathbf{X}_i + \mathbf{X}_{i+1}) / 2 \quad (2)$$

$$\begin{aligned} \mathbf{l}_1 &= \frac{(\mathbf{X}_{side1} - \mathbf{X}_{side3})}{\|(\mathbf{X}_{side1} - \mathbf{X}_{side3})\|} \\ \mathbf{l}_2 &= \frac{(\mathbf{X}_{side2} - \mathbf{X}_{side4})}{\|(\mathbf{X}_{side2} - \mathbf{X}_{side4})\|} \end{aligned} \quad (3)$$

The local coordinate vectors  $V_r$ ,  $V_s$ ,  $V_t$  are the found by

$$\begin{aligned} \mathbf{V}_t &= \mathbf{l}_1 \times \mathbf{l}_2 \\ \mathbf{V}_s &= \frac{[(\mathbf{V}_t \times \mathbf{l}_1) + \mathbf{l}_2]}{\|(\mathbf{V}_t \times \mathbf{l}_1) + \mathbf{l}_2\|} \\ \mathbf{V}_r &= \mathbf{V}_s \times \mathbf{V}_t \end{aligned} \quad (4)$$

and the local coordinates of node  $i$  is

$$\begin{Bmatrix} r \\ s \\ t \end{Bmatrix}_i = [\mathbf{V}_r \quad \mathbf{V}_s \quad \mathbf{V}_t]^T (\mathbf{X}_i - \mathbf{X}_c) = \mathbf{T}^T (\mathbf{X}_i - \mathbf{X}_c) \quad (5)$$

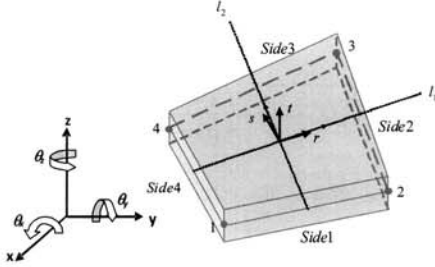


Fig 1. Mid-Surface Geometry and Local Coordinates of 4 node Shell element

Having defined the local coordinate base vectors, the transformation of the incremental displacement parameters  $\Delta \bar{\mathbf{u}}_i$ ,  $\Delta \bar{\boldsymbol{\varphi}}_i$  at node  $i$  from the element local coordinates, to the global coordinates, is done by

$$\begin{Bmatrix} \Delta \bar{\mathbf{u}} \\ \Delta \bar{\boldsymbol{\varphi}} \end{Bmatrix}_i = \begin{Bmatrix} \mathbf{T}^T & \mathbf{0} \\ \mathbf{0} & \mathbf{T}^T \end{Bmatrix} \begin{Bmatrix} \Delta \bar{\mathbf{U}}_i \\ \Delta \bar{\mathbf{V}}_i \\ \Delta \bar{\mathbf{W}}_i \\ \Delta \theta_{xi} \\ \Delta \theta_{yi} \\ \Delta \theta_{zi} \end{Bmatrix} = \mathbf{T}_s^T \begin{Bmatrix} \Delta \bar{\mathbf{U}} \\ \Delta \bar{\boldsymbol{\theta}} \end{Bmatrix}_i \quad (6)$$

Transformation matrix  $\mathbf{T}$  is defined as

$$\mathbf{T} = \begin{bmatrix} l_r & l_s & l_t \\ m_r & m_s & m_t \\ n_r & n_s & n_t \end{bmatrix} = [\mathbf{V}_r \quad \mathbf{V}_s \quad \mathbf{V}_t] \quad (7)$$

It is important to note that  $\mathbf{V}_t$  is normal to the mid-surface of the element and it is independent of the top and the bottom nodal coordinates.

### 3. Strain-Displacement Relationships

The local kinematic relations based on the co-rotational displacement can be expressed as Follows:

$$\begin{aligned} \Delta \hat{\mathbf{u}} &= \Delta \hat{\bar{\mathbf{u}}} + \mathbf{t} \left( \Delta \hat{\boldsymbol{\varphi}}_s + \frac{1}{2} \Delta \hat{\boldsymbol{\varphi}}_r \Delta \hat{\boldsymbol{\varphi}}_t \right) \\ \Delta \hat{\mathbf{v}} &= \Delta \hat{\bar{\mathbf{v}}} - \mathbf{t} \left( \Delta \hat{\boldsymbol{\varphi}}_r - \frac{1}{2} \Delta \hat{\boldsymbol{\varphi}}_s \Delta \hat{\boldsymbol{\varphi}}_t \right) \\ \Delta \hat{\mathbf{w}} &= \Delta \hat{\bar{\mathbf{w}}}(\mathbf{r}, s) \end{aligned} \quad (8)$$

The linear and non-linear part of the local incremental Green strain can be determined using the kinematic relation expressed in Eq. (8). In the quasi-conforming technique (QCT), the element strain fields are approximated using polynomials and are integrated using string functions or boundary displacement interpolation functions. The starting point of the quasi-conforming element is to interpolate element strain fields in terms of the undetermined strain parameters. Strains  $\Delta \hat{\boldsymbol{\epsilon}}$  is approximated as

$$\Delta \hat{\boldsymbol{\epsilon}} \approx \mathbf{P} \Delta \boldsymbol{\alpha} \approx \mathbf{B} \begin{Bmatrix} \Delta \hat{\bar{\mathbf{u}}} \\ \Delta \hat{\boldsymbol{\varphi}} \end{Bmatrix} \quad (9)$$

where  $\mathbf{P}$  are chosen strain interpolation polynomial functions,  $\Delta \boldsymbol{\alpha}$  are undetermined strain parameters and  $\mathbf{B}$  is the strain-displacement matrix. Letting  $\mathbf{W}$  be the test function, then

$$\int_{\Omega} \mathbf{W} (\Delta \hat{\boldsymbol{\epsilon}} - \mathbf{P} \Delta \boldsymbol{\alpha}) d\Omega = 0 \quad (10)$$

would be the weak form. The test function is taken as  $\mathbf{W} = \mathbf{P}^T$ .  $\Delta \boldsymbol{\alpha}$  can then be determined by carrying out the integration.

$$\Delta \boldsymbol{\alpha} = \mathbf{A}^{-1} \mathbf{G} \begin{Bmatrix} \Delta \hat{\bar{\mathbf{u}}} \\ \Delta \hat{\boldsymbol{\varphi}} \end{Bmatrix} \quad (11)$$

where

$$\mathbf{A} = \int_{\Omega} (\mathbf{P}^T \mathbf{P}) d\Omega \quad \text{and} \quad \mathbf{G} \begin{Bmatrix} \Delta \hat{\mathbf{u}} \\ \Delta \hat{\boldsymbol{\phi}} \end{Bmatrix} = \int_{\Omega} (\mathbf{P}^T \Delta \hat{\boldsymbol{\epsilon}}) d\Omega \quad (12)$$

Substituting a in (11) to (9) defines the strains in terms of the element displacements.

$$\Delta \hat{\boldsymbol{\epsilon}} = \mathbf{B} \begin{Bmatrix} \Delta \hat{\mathbf{u}} \\ \Delta \hat{\boldsymbol{\phi}} \end{Bmatrix} = \mathbf{P} \mathbf{A}^{-1} \mathbf{G} \begin{Bmatrix} \Delta \hat{\mathbf{u}} \\ \Delta \hat{\boldsymbol{\phi}} \end{Bmatrix} \quad (13)$$

In terms of the global displacement vector, equation (13) is written as

$$\Delta \hat{\boldsymbol{\epsilon}} = \mathbf{B} \mathbf{T}_g^T \begin{Bmatrix} \Delta \hat{\mathbf{U}} \\ \Delta \hat{\boldsymbol{\theta}} \end{Bmatrix} = \mathbf{P} \mathbf{A}^{-1} \mathbf{G} \mathbf{T}_g^T \begin{Bmatrix} \Delta \hat{\mathbf{U}} \\ \Delta \hat{\boldsymbol{\theta}} \end{Bmatrix} \quad (14)$$

$\mathbf{T}_g$  is a diagonal matrix composed of T defined in equation (7).  $\Delta \hat{\mathbf{U}}$  and  $\Delta \hat{\boldsymbol{\theta}}$  are global displacement vectors. Using the relation of strain-displacement defined above, the element stiffness can be determined.

#### 4. Elasto-plastic materials using Ivanov's yield criterion with isotropic hardening

The present shell element uses resultant membrane forces (N), moments (M) and transverse shear forces (Q) in obtaining the integration of stresses through the thickness. Ivanov's yield criteria which was suggested by Crisfield [5] relates to the six resultant forces and moments in a shell element ( $N_r, N_s, N_{rs}, M_r, M_s, M_{rs}$ ). It is extended to take into account the isotropic hardening effects. The major advantage of this formulation is significantly less time consuming when the stiffness matrix and internal load vector are formulated by pre-integration through the thickness. In the

formulation of Ivanov's yield criterion, the predictor corrector method with sub increments is used.

The following Ivanov's yield criterion, f will give more accurate approximation than Ilyushin's [4] full section yield surface by using higher order terms in the yield function.

$$f = Q'_i + \frac{1}{2} Q'_m + \sqrt{\frac{1}{4} Q_m'^2 + Q_{tm}'^2} - \frac{1}{4} \frac{(Q'_i Q'_m - Q_{tm}'^2)}{(Q'_i + 0.48 Q'_m)} - \sigma_y^2 \quad (15)$$

Where,  $Q'_i, Q'_m, Q'_{tm}$  are the quadratic stress intensities.

$$Q'_i = \frac{\bar{N}}{t^2}, \quad Q'_m = \frac{16\bar{M}}{\alpha^2 t^4}, \quad Q'_{tm} = \frac{4\bar{M}\bar{N}}{\alpha t^3} \quad (16)$$

$$\bar{N} = N_r^2 + N_s^2 - N_r N_s + 3N_{rs}^2 \quad (17)$$

$$\bar{M} = M_r^2 + M_s^2 - M_r M_s + 3M_{rs}^2 \quad (18)$$

$$\bar{M}\bar{N} = M_r N_r + M_s N_s - \frac{1}{2} M_r N_s - \frac{1}{2} M_s N_r + 3M_{rs} N_{rs} \quad (19)$$

$$\mathbf{N} = \{N_r, N_s, N_{rs}\}, \quad \mathbf{M} = \{M_r, M_s, M_{rs}\} \quad (20)$$

$$\mathbf{M}_o = \frac{1}{4} \sigma_y t^2, \quad \mathbf{N}_o = \sigma_y t \quad (21)$$

Where,  $\sigma_y$  is uni-axial yield stress and t is the shell thickness.

In the predictor corrector method, the incremental stress resultant force (trial) can be calculated by assuming the elastic loading as follow:

$$\begin{Bmatrix} \Delta \mathbf{N} \\ \Delta \mathbf{M} \end{Bmatrix} = \mathbf{D}^e \begin{Bmatrix} \Delta \hat{\boldsymbol{\epsilon}}_m \\ \Delta \hat{\boldsymbol{\kappa}} \end{Bmatrix} \quad (22)$$

Where,  $\mathbf{D}^e$  is the elastic strain stress rigidity matrix after integrating through the thickness.

During an increment of the resultant forces and moments, the elastic predictor stress resultant vector may bring the stress state outside the yield surface. The computation of contact stress state (transition from elastic to plastic behaviour) is

needed to find the amount of elastic strain increment. The factor  $r$  which is approximated as 'a factor-  $r$ ' times the total incremental strain is required to find the strain increments that caused the stresses that have reached the yield surface (only due to elastic loading).

At the contact stress state, the yield function  $\mathbf{f} = \mathbf{f}(Q_t^s, Q_m^s, Q_{tm}^s, \sigma_y) = 0$ . Therefore, the factor  $r$  can be determined by solve the following equation:

$$\mathbf{f}(Q(\mathbf{N} + r\Delta\mathbf{N}), Q_m^s(\mathbf{M} + r\Delta\mathbf{M}), Q_{tm}^s(\mathbf{M} + r\Delta\mathbf{M}, \mathbf{N} + r\Delta\mathbf{N}), \sigma_y) = 0 \quad (23)$$

By means of associate flow rule, the direction of the plastic strains are assumed to be normal to the yield surface, which can be determine by differentiate the yield surface. Applying the chain rule the normal vector can be derived as follows:

$$\delta\mathbf{f} = \frac{\partial\mathbf{f}}{\partial\mathbf{N}}\Delta\mathbf{N} + \frac{\partial\mathbf{f}}{\partial\mathbf{M}}\Delta\mathbf{M} + \frac{\partial\mathbf{f}}{\partial\alpha} \frac{\partial\alpha}{\partial\hat{\kappa}_{eps}} \Delta\hat{\kappa}_{eps} + \frac{\partial\mathbf{f}}{\partial\sigma_y} \frac{\partial\sigma_y}{\partial\hat{\mathbf{e}}_e^p} \Delta\hat{\mathbf{e}}_e^p \quad (24)$$

$$\mathbf{f}_N^T \Delta\mathbf{N} + \mathbf{f}_M^T \Delta\mathbf{M} + \frac{\partial\mathbf{f}}{\partial\alpha} \frac{\partial\alpha}{\partial\hat{\kappa}_{eps}} \Delta\hat{\kappa}_{eps} + \frac{\partial\mathbf{f}}{\partial\sigma_y} \frac{\partial\sigma_y}{\partial\hat{\mathbf{e}}_e^p} \Delta\hat{\mathbf{e}}_e^p = 0 \quad (25)$$

Where  $\Delta\hat{\mathbf{e}}_e^p$  is the incremental effective plastic strain.

The derivatives of yield function used in Eq. (24) and (25),  $\mathbf{f}_N = \frac{\partial\mathbf{f}}{\partial\mathbf{N}}$ ,  $\mathbf{f}_M = \frac{\partial\mathbf{f}}{\partial\mathbf{M}}$ ,  $\frac{\partial\mathbf{f}}{\partial\alpha}$  and  $\frac{\partial\alpha}{\partial\hat{\kappa}_{eps}}$  can be calculated as follows:

$$\mathbf{f}_N = \left[ 1 - \frac{1}{4} \frac{Q_m^s}{(Q_t^s + 0.48Q_m^s)} + \frac{1}{4} \frac{(Q_t^s Q_m^s - Q_{tm}^s)^2}{(Q_t^s + 0.48Q_m^s)^2} \right] \frac{\partial Q_t^s}{\partial \mathbf{N}} + Q_m^s \left( \frac{1}{\sqrt{4} Q_m^s + Q_{tm}^s} + \frac{1}{2(Q_t^s + 0.48Q_m^s)} \right) \frac{\partial Q_m^s}{\partial \mathbf{N}} \quad (26)$$

$$\mathbf{f}_M = \left[ \frac{1}{2} \frac{1}{4} \frac{Q_m^s}{\sqrt{4} Q_m^s + Q_{tm}^s} - \frac{1}{4} \frac{Q_t^s}{(Q_t^s + 0.48Q_m^s)} + 0.12 \frac{(Q_t^s Q_m^s - Q_{tm}^s)^2}{(Q_t^s + 0.48Q_m^s)^2} \right] \frac{\partial Q_t^s}{\partial \mathbf{M}} + Q_m^s \left( \frac{1}{\sqrt{4} Q_m^s + Q_{tm}^s} + \frac{1}{2(Q_t^s + 0.48Q_m^s)} \right) \frac{\partial Q_m^s}{\partial \mathbf{M}} \quad (27)$$

$$\frac{\partial\mathbf{f}}{\partial\alpha} = \left[ \frac{1}{2} + \frac{1}{4} \frac{Q_m^s}{\sqrt{4} Q_m^s + Q_{tm}^s} - \frac{1}{4} \frac{Q_t^s}{(Q_t^s + 0.48Q_m^s)} + 0.12 \frac{(Q_t^s Q_m^s - Q_{tm}^s)^2}{(Q_t^s + 0.48Q_m^s)^2} \right] \frac{\partial Q_t^s}{\partial\alpha} + Q_m^s \left( \frac{1}{\sqrt{4} Q_m^s + Q_{tm}^s} + \frac{1}{2(Q_t^s + 0.48Q_m^s)} \right) \frac{\partial Q_m^s}{\partial\alpha} \quad (28)$$

$$\frac{\partial\alpha}{\partial\hat{\kappa}_{eps}} = \frac{0.52}{\sqrt{\hat{\kappa}_{eps}}} \left( \frac{Et}{3\sigma_0} \right)^{\frac{1}{2}} \text{Exp}^{(-2.6)\sqrt{\hat{\kappa}_{eps}}} \quad (29)$$

Therefore, the incremental plastic strain can be determined as follows:

$$\Delta\hat{\mathbf{e}}_s^p = \Delta\lambda \mathbf{f}_N$$

$$\Delta\hat{\kappa}_s^p = \Delta\lambda \mathbf{f}_M \quad (30)$$

where  $\Delta\lambda$  is the plastic strain multiplier which can be calculate using concept of plastic work done:

$$\Delta\lambda = \frac{\sigma_y \Delta\hat{\mathbf{e}}_e^p}{\mathbf{N}^T \mathbf{f}_N + \mathbf{M}^T \mathbf{f}_M} \quad (31)$$

where,  $\Delta\hat{\mathbf{e}}_e^p$  is an effective stress and effective incremental plastic strain.

The effective plastic strain increment  $\Delta\hat{\mathbf{e}}_e^p$  can be calculated by substituting Eq. (26)-(29), (30) and (31) into Eq. (25).

$$\Delta\hat{\mathbf{e}}_e^p = \frac{(\mathbf{N}^T \mathbf{f}_N + \mathbf{M}^T \mathbf{f}_M)}{\sigma_y \left[ m1 + n1 + 11 - \mathbf{B} \frac{\partial\mathbf{f}}{\partial\alpha} \frac{\partial\alpha}{\partial\hat{\kappa}_{eps}} \right]} \left( \mathbf{t} \mathbf{f}_N^T \mathbf{D}^s \Delta\hat{\mathbf{e}}_t^s + \frac{t^3}{12} \mathbf{f}_M^T \mathbf{D}^s \Delta\hat{\kappa}_t^s \right) \quad (32)$$

$$11 = 2h(\mathbf{N}^T \mathbf{f}_N + \mathbf{M}^T \mathbf{f}_M), m1 = \frac{t^3}{12} \mathbf{f}_M^T \mathbf{D}^s \mathbf{f}_M, n1 = \mathbf{t} \mathbf{f}_N^T \mathbf{D}^s \mathbf{f}_N \quad (33)$$

where, the superscript  $t$  indicate the total strain components.

The elastic incremental stress resultant forces-strain laws are assumed to be linear in nature and by applying it, incremental stress resultant forces

can be calculated as follows

$$\begin{aligned} \Delta \mathbf{N} &= {}^t \mathbf{D}^e \left[ \Delta \hat{\mathbf{e}}_s^t - \Delta \hat{\mathbf{e}}_s^p \right] \\ \Delta \mathbf{M} &= \frac{t^3}{12} \mathbf{D}^e \left[ \Delta \hat{\boldsymbol{\kappa}}_s^t - \Delta \hat{\boldsymbol{\kappa}}_s^p \right] \end{aligned} \quad (34)$$

Substituting the plastic strain increments in Eq. (30), (31) and (32) into Eq. (34), the constitutive relationship between the increments of the stress resultant forces and moments, and the increments of total strain increment that governs the plasticity can be formulated as follows:

$$\begin{Bmatrix} \Delta \mathbf{N} \\ \Delta \mathbf{M} \end{Bmatrix} = \begin{bmatrix} \mathbf{C}^1 & \mathbf{C}^2 \\ \mathbf{C}^2 & \mathbf{C}^3 \end{bmatrix} \begin{Bmatrix} \Delta \hat{\mathbf{e}}_s^t \\ \Delta \hat{\boldsymbol{\kappa}}_s^t \end{Bmatrix} \quad (35)$$

Where the tangential elasto-plastic modular matrices considering the isotropic strain hardening can be defined as follows:

$$\begin{aligned} \mathbf{C}^1 &= {}^t \mathbf{D}^e \left[ \mathbf{I} - \frac{{}^t \mathbf{f}_N \mathbf{f}_N^T \mathbf{D}^e}{ml + nl + ll - \tilde{\mathbf{B}} \frac{\partial \mathbf{f}}{\partial \alpha} \frac{\partial \alpha}{\partial \hat{\boldsymbol{\kappa}}_{ps}}} \right] \\ \mathbf{C}^2 &= - \frac{{}^t \mathbf{D}^e \mathbf{f}_N \mathbf{f}_M^T \mathbf{D}^e}{12 \left[ ml + nl + ll - \tilde{\mathbf{B}} \frac{\partial \mathbf{f}}{\partial \alpha} \frac{\partial \alpha}{\partial \hat{\boldsymbol{\kappa}}_{ps}} \right]} \\ \mathbf{C}^3 &= \frac{t^3}{12} \mathbf{D}^e \left[ \mathbf{I} - \frac{{}^t \mathbf{f}_M \mathbf{f}_M^T \mathbf{D}^e}{12 \left[ ml + nl + ll - \tilde{\mathbf{B}} \frac{\partial \mathbf{f}}{\partial \alpha} \frac{\partial \alpha}{\partial \hat{\boldsymbol{\kappa}}_{ps}} \right]} \right] \end{aligned} \quad (36)$$

## 5. EQUATION OF MOTION

In formulating the new shell element, an updated Lagrangian formulation was adopted. The linearized equation of motion, is expresses as

$$\int_V {}^t C_{ijkl} \Delta e_{ij} \delta \Delta e_{kl} d^3V + \int_V {}^t \tau_{ij} \delta \Delta \Xi_{ij} d^3V = {}^{t+\Delta t} \mathfrak{R} - \int_V {}^t \tau_{ij} \delta \Delta e_{ij} d^3V \quad (37)$$

$C_{ijrs}$  is the component of the constitutive tensor,  ${}^t \tau_{ij}$  is the component of the Cauchy stress tensor,  ${}^{t+\Delta t} \mathfrak{R}$  is the external virtual work expression, and  $\Delta e_{ij}$  and  $\Delta \Xi_{ij}$  are the incremental linear and nonlinear part of the strain tensor, respectively.

Assuming constant thickness during deformation, (37) may be expressed as

$$\begin{aligned} & \sum_{elem} \int_{\Omega} \left[ (\delta \Delta e_m^t \mathbf{A} \Delta e_m + \delta \Delta e_n^t \mathbf{B} \Delta e_n + \delta \Delta e_o^t \mathbf{B} \Delta e_o + \delta \Delta e_p^t \mathbf{D} \Delta e_p + \delta \Delta e_q^t \bar{\mathbf{A}} \Delta e_q) dr ds \right] + \\ & \sum_{elem} \int_{\Omega} \left[ (\mathbf{N}^T \delta \Delta \Xi_m + \mathbf{M}^T \delta \Delta \Xi_n + \mathbf{Q}^T \delta \Delta \Xi_o) dr ds \right] = {}^{t+\Delta t} \mathfrak{R} \\ & - \sum_{elem} \int_{\Omega} \left[ (\delta \Delta e_b^t \mathbf{M} + \delta \Delta e_m^t \mathbf{N} + \delta \Delta e_q^t \mathbf{Q}) dr ds \right] \end{aligned} \quad (38)$$

## 6. Numerical Example

The present nonlinear formulation of 4-node quasi-conforming shell element (XSHELL-4QSI) is implemented into the general purpose Nonlinear Dynamic Finite Element Package, XFINAS, developed in AIT, for the PC. XFINAS is an extended version of the nonlinear finite element package FINAS, developed in Imperial College, London. Results to the analysis of static non-linear problems using XSHELL-4-QSI is presented to validate the numerical performance of the nonlinear formulation. The Window version of XFINAS runs on a personal computer with Graphical software GiD developed by CIMNE.

### 6.1 Large-deflection elasto-plastic analysis of an imperfect rectangular plate under in-plane loading

A simply supported plate subjected to in-plane loading is analyzed. The plate undergoes both large deflections and plasticity. An initial out-of-plane imperfection was created equivalent to  $w = w_o \sin(\pi x/a) \sin(\pi y/b)$ . Because of symmetry, only one quarter of the plate was used in the model

with an 5x5mesh. The tolerance for convergence used was 0.0005. Twelve displacement increments were used with a maximum of 2 iterations of MNR per increment. This makes the present formulation more efficient than the reference by Javaherian and Dowling [9] used for comparison, which used a tolerance of 0.003, 15 displacement increments for the same total displacement and a maximum of 5 MNR iterations per increment.

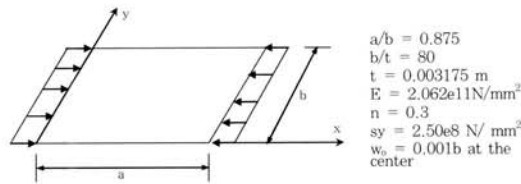


Fig 2. Plate geometry and material properties.

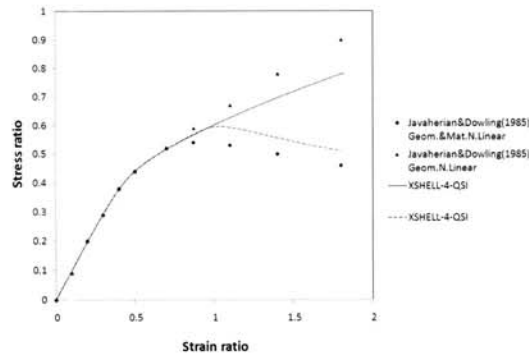


Fig 3. Normalized average in-plane stress vs. average in-plane strain.

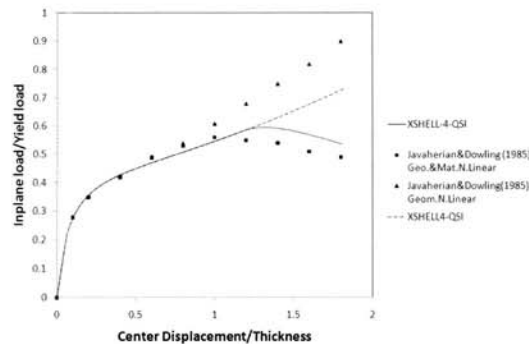


Fig 4. Normalized Out-of-Plane Force-Displacement Diagram

## 6.2 Large-deflection elasto-plastic analysis of discretely stiffened plate under in-plane loading.

A stiffened flat plate subjected to in-plane loading was analysed. Only half of the stiffened plate was analysed because of symmetry. A mesh of 16x12 was made for the plate and 4x12 for the stiffeners. Plasticity assumption is the same as that of Webb and Dowling [11]. A full depth yield criterion was used for the plate while stiffeners are of multi-layer approach. The solution obtained are plotted with those of Webb and Dowling [11] and Dhajani [10] whose solutions were based on finite difference. A test result for the same plate indicates a normalized peak load of 1.009. The difference between the present analysis and the test results may be attributed to the residual stresses and actual imperfections of the specimen.

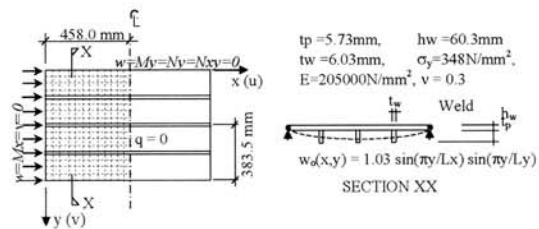


Fig 5. Stiffened plate geometry and material properties.

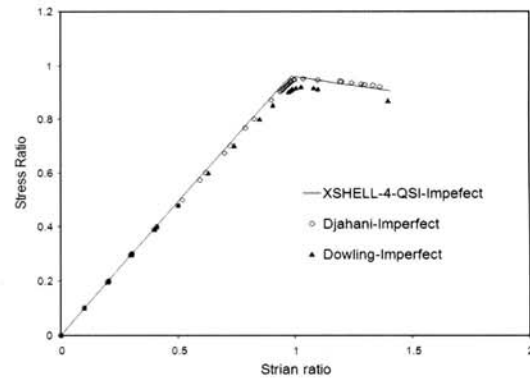


Fig 6. Normalized average in-plane stress vs. average in-plane strain of stiffened plate. Inset: deformed shape (x10) with in-plane stress contour.

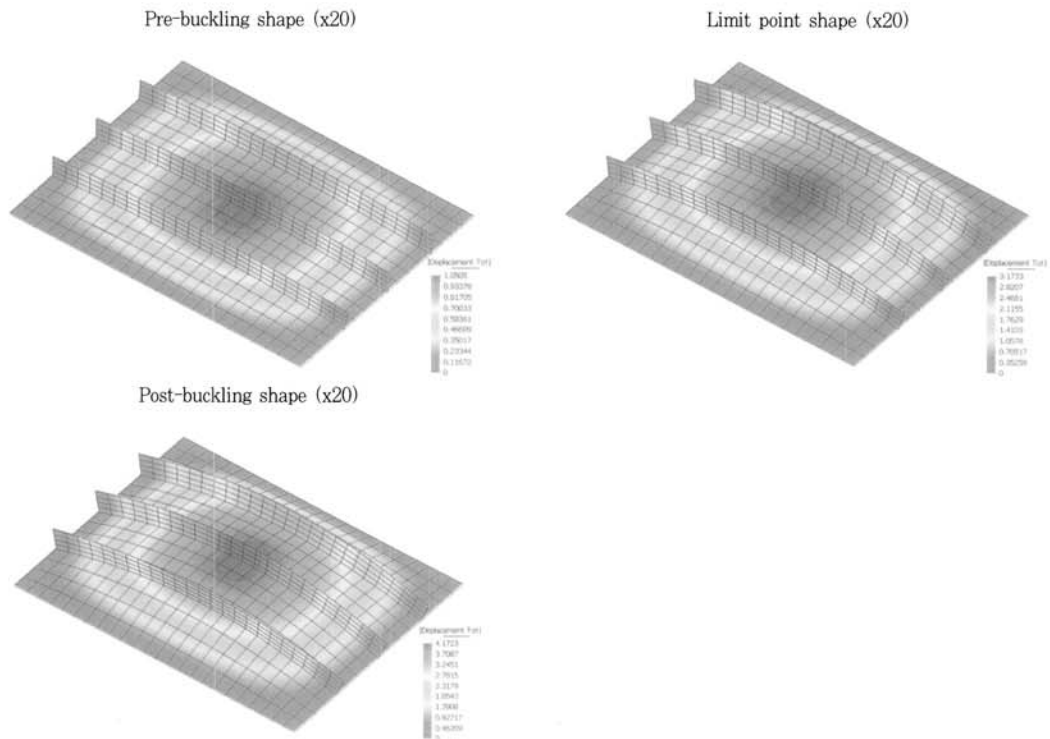


Fig 7. Deformed shape of stiffened plate under axial compression

### 6.3 Elasto-plastic Buckling of Imperfect Stiffened Curved Panel

The choice of a suitable imperfection shape is the most difficult task in the postbuckling analysis of shell structures. In order to identify the imperfection sensitivity of stringer stiffened shells under axial and pressure loading, Agelidis [12] carried out a large parametric study of stiffened cylindrical shell covering a broad range of geometries used in the offshore structural engineering. In the following, an imperfect stiffened curved panel subjected to inplane loading is analyzed. The model adopted is Agelidis panel widely used for steel shell buckling problem, in Imperial College, London. Considering large deformation elasto-plastic analysis of one octant of a cylinder with stiffener, the stiffened panel was modeled with 96 shell elements.

For comparison, the results with XSELLA-QSI were plotted with those obtained using the 8-node co-rotational element (XSELL8-ANS). For the 8-node elements, the stiffened panel was model using 24 elements as shown in Fig. 8. The pre and post buckling behaviour of the panel are similarly predicted by both elements.

In this study, assuming an odd number of half waves for the deflection in the longitudinal direction only of the half panel between the rings was modeled. In the present study, it was decided to select imperfection shapes determined from a single half sine wave in circumferential and longitudinal directions. The numerical 'knockdown' factor (defined here as the limit load obtained from non-linear analysis) is 0.51 for an imperfection amplitude equal to 10% of the thickness.



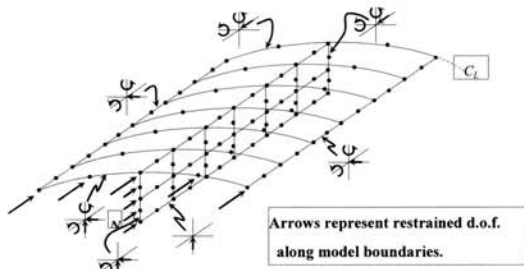


Fig 8. Geometry of Stiffened Curved Panel

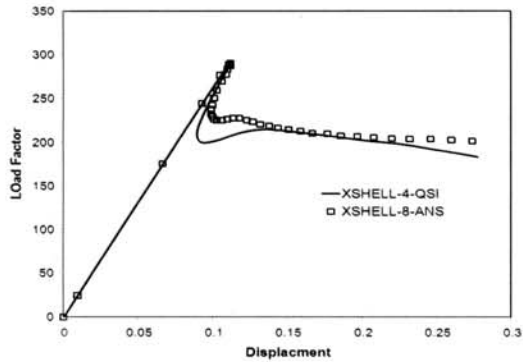


Fig 9. Load-deflection curve of Stiffened Curved Panel

#### 6.4 Pinched Elasto-Plastic Cylinder with Isotropic Hardening

A thin cylinder, pinched at the mid sections is analyzed for large displacement, rotation and elasto-plastic behaviour. Two methods have been used for the analysis, elasto-plastic with Ivanov and elasto-plastic multilayer with Von Mises yield criterion with isotropic hardening. The cylinder has two end diaphragms. It was modeled using only one octant with a 32X32 mesh of four-node elements. The cylinder geometry and material properties are shown in Figure 11. The solution by Simo and Kennedy [13] using generalized Ilyushin-Shapiro elastoplastic model and Brank, et al. [14] using von Mises yield criterion with seven integration points are also shown with the present results, Figure 12. The same snap-through response observed by Brank, et al. is also seen in the present analysis with similar limit points and stiffening behaviour. The geometry at different stages of deformation is shown in Fig.13

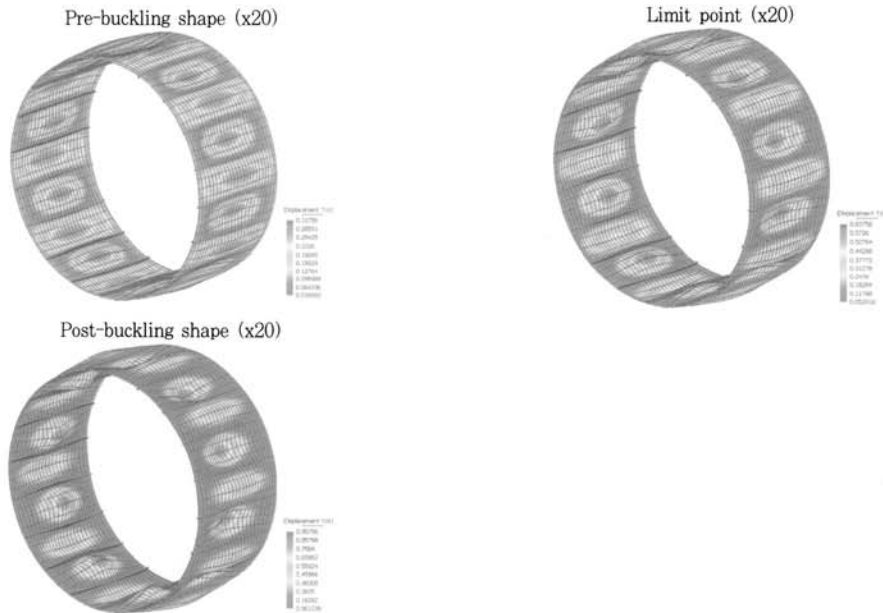


Fig 10. Deformed shape of elasto-plastic stiffened cylinder under axial compression

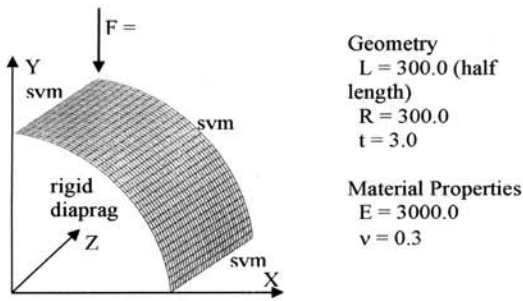


Fig 11. Pinched elasto-plastic cylinder- geometry and materials properties

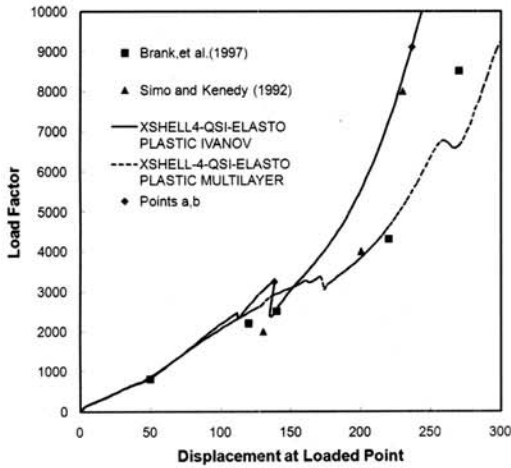


Fig 12. Pinched elasto-plastic cylinder-displacement under force

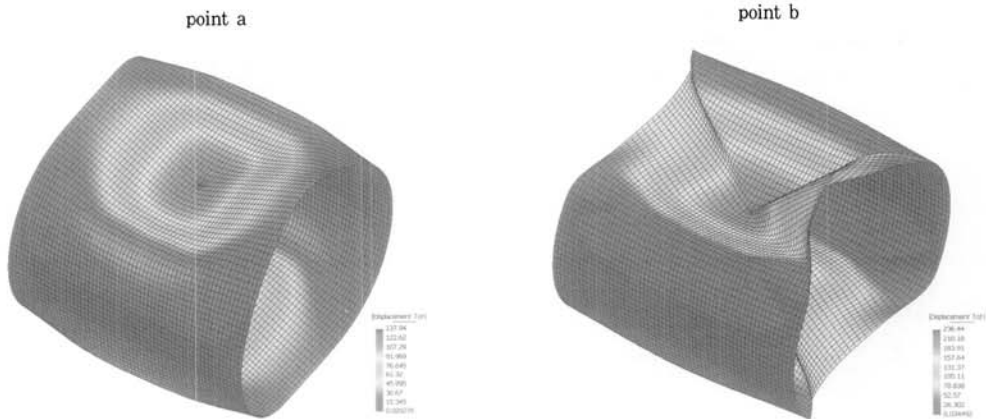


Fig 13. Pinched elasto-plastic cylinder- deformed configuration

## 7. Concluding Remarks

The nonlinear formulation of shell element is already developed through the quasi-conforming technique. The highlight of the quasi-conforming technique is not to use numerical integration but to use explicit integration and obtain stresses at the nodal points accurately. All the nonlinear problems which use the co-rotational method converge very well and show the full load-deflection curves. The present resultant shell element involving pre-integration through the thickness takes into account of the explicit plasticity of Ivanov's yield condition with isotropic strain hardening. By avoiding the multi-layer integrations, this method is computationally very efficient in the large scale of plastic modeling of the thin shell structures. The load-deflection curve and deformed shape show very good performance with references.

## 감사의 글

이 연구는 건설교통부 한국건설기술평가원의 건설혁신기술 연구개발사업(06건설핵심D05) 지원에 의하여 이루어졌으며, 저자들은 이에 감사를 드립니다.

REFERENCES

Simo J.C. and Rifai M.S., 1990. A class of mixed assumed strain method of incompatible modes. *International Journal for Numerical Methods in Engineering*, 29:1595-1638.

Shi, G., and Voyiadjis, G.Z., 1991. Geometrically Nonlinear Analysis of Plates by Assumed Strain Element with Explicit Tangent Stiffness Matrix. *Computers and Structures*, 41:757-763.

Voyiadjis, G.Z., and Shi, G., 1992. Nonlinear Post-Buckling Analysis of Plates and Shallow Shells by Four-Noded Quadrilateral Strain Element. *AIAA Journal*, 30(4):1110-1116.

A.A. Ilyushin, Plasticitie, Editions Eyrolles, Paries, 1956.

M.A. Crisfield, On an approximate yield criterion for thin steel shell, Internal Report, Crowthorne, Berkshire TRRL, 1974.

Q. Zeng, A. Comdescure, F. Arnaudean, An efficient plasticity algorithm for shell elements application to metal forming simulation, *Computers and Struct.* (2001) pp. 1525-1540.

K.D. Kim, G.R. Lomboy and G.Z.Voyiadjis, A 4-Node Assumed Strain Quasi-Conforming Shell Element with 6 D.O.F., *International Journal for Numerical Methods in Engineering*, Volume 58, Issue 14, pp. 2177-2200, December 2003

K.D.Kim, G.R. Lomboy, A Co-rotational Quasi-Conforming 4-Node Assumed Strain Shell Element for Large Displacement of Elasto-plastic Analysis, *Computer Methods in Applied Mechanics and Engineering*, 195 (2006) pp. 6502-6522, September

Javaherian H. and Dowling P.J. (1985), Large deflection elasto-plastic analysis of thin shells, *Enging Struct.* Vol.7 July, pp. 154-162.

Djhani P. (1977), Large deflection elasto-plastic analysis of discretely stiffened plates, Ph.D. Thesis, Dept. of Civil Engineering, Imperial College, London.

Webb S.E. and Dowling P.J. (1980), Large-deflection elasto-plastic behaviour of discretely stiffened plates, *Proceeding of Institutions of Civil Engineers*, Part 2, 69, 3 June pp. 75-401.

Agelidis, N. (1984), Buckling of stringer stiffened shells under axial and pressure loading, Ph.D. Thesis, Dept. of Civil Engineering, Imperial College, London.

J.C. Simo, J.G. Kennedy, On a stress resultant geometrically exact shell model Part V: Nonlinear plasticity: Formulation and integration algorithm, *Comput. Methods Appl. Mech. Eng.* 96 (1992) pp. 133-171.

B. Brank, D. Peric, F.B. Damjanic, On large deformation of thin elasto-plastic shells: implementation of finite rotation model for a quadrilateral shell element, *Int. J. Numer. Methods Eng.* 40 (1997) pp. 689-726.

(접수일자 : 2008. 4. 15 / 심사일 2008. 4. 21 / 게재확정일 2008. 4. 24)